Zintl Ions Blossom out ...

The "bud" of $[In_4Bi_5]^{3-}$

+ 7e-

and the blossomed 'one electron deficient' $[In_4Bi_5]^{10-}$ cluster

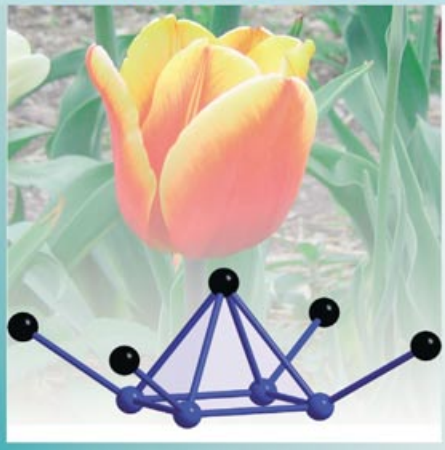

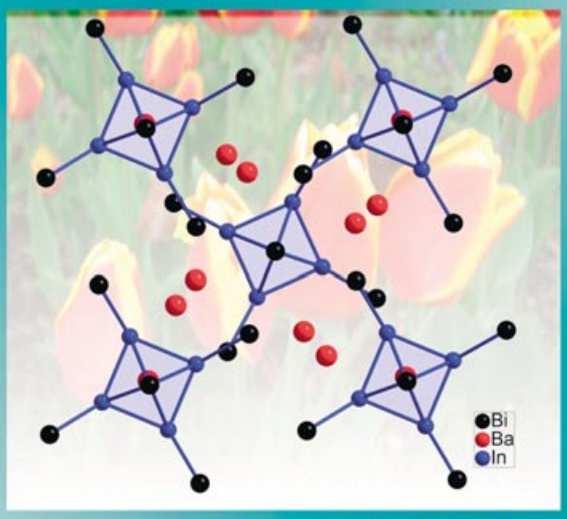

Interconnected $[In_4Bi_5]^{10-}$ clusters in $Ba_5In_4Bi_5$ crystal structure...

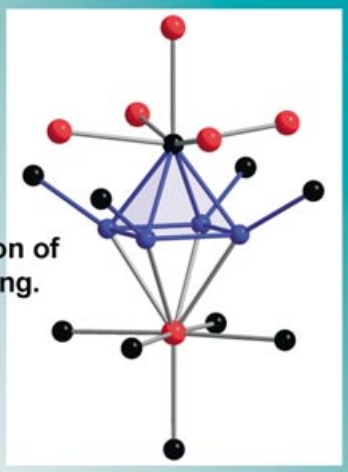

... with substantial contribution of Ba atoms to the overall bonding.

For more details read on...

 DOI: 10.1002/chem.200306061

Synthesis, Characterization, and Electronic Structure of $Ba_5In_4Bi_5$: An Acentric and One-Electron Deficient Phase

Siméon Ponou,[a] Thomas F. Fässler,*[a] Gerard Tobías,[b] Enric Canadell,*[b] Ara Cho,[c] and Slavi C. Sevov*[c]

Abstract: The new ternary phase $Ba_5In_4Bi_5$ was synthesized by direct reaction of the corresponding elements at high temperature. It crystallizes in a noncentrosymmetric space group and represents a new structure type (tetragonal, *P4nc* with $a = 10.620(2)$ and $c = 9.009(2)$ Å, $Z = 2$). The structure is built of interconnected heteroatomic clusters of In_4Bi_5, square pyramids with In_4-bases and four *exo*-bonded bismuth atoms (bond to the In atoms). According to Wade's rule the compound is electron-deficient with one electron per cluster, that is, $[In_4Bi_5]^{10-}$ instead of the expected $[In_4Bi_5]^{11-}$ for a closed-shell species. The clusters are discussed also in light of the known heteroatomic deltahedral clusters with the same composition but different charge, $[In_4Bi_5]^{3-}$. Band structure calculations on the new compound suggest substantial participation of barium in the overall bonding of the structure that "accounts" for the electron shortage

Keywords: barium · cluster compounds · pnictides · solid-state structures

Introduction

Reduction of the heavier main-group p elements by alkali and alkaline-earth metals produces polar intermetallics that contain various polyanions of those elements. Such compounds are rationalized by the Zintl–Klemm concept as ionic compounds, in which the more electropositive metals lose their valence electrons to the more electronegative p elements.[1] The transferred electrons, however, are often not enough for the p elements to achieve octets as isolated anions and, instead, they are "forced" to form bonds to each other. The resulting polyatomic species may be homo- or heteroatomic and may have various sizes and dimensions. Many such formations are known for heteroatomic anions involving atoms of Groups 13 (triels, Tr = Al, Ga, In, Tl) and 15 (pnictogens, Pn = P, As, Sb, Bi), $[Tr_mPn_n]^{q-}$. One of the most common motifs is $TrPn_4$, a tetrahedrally coordinated triel atom. Isolated tetrahedra, $[TrPn_4]^{9-}$, dimers of edge-bridged tetrahedra, $[Tr_2Pn_6]^{12-}$, chains of corner-shared tetrahedra, $_\infty^1[TrPn_3]^{6-}$, chains of edge-shared tetrahedra, $_\infty^1[TrPn_2]^{3-}$, layers and 3D-frameworks of corner- and edge-shared tetrahedra and many other combinations of variously shared tetrahedra are known.[2] Often the tetrahedra are connected through Pn–Pn bonds[2] and very rarely even by Tr–Tr bonds.[3] Trigonal-planar coordination ($TrPn_3$) is also known and the units have been found as isolated $[TrPn_3]^{6-}$, edge-sharing in dimers of $[Tr_2Pn_4]^{6-}$, and corner-sharing in a ring-like trimer of $[Tr_3Pn_6]^{9-}$.[2a]

Recent studies, however, have revealed that often the anionic substructures of such compounds are far more diverse and beyond the grasp of the original Zintl–Klemm concepts. Transition-metal Zintl phases[4] and some with mixed valency,[5] as well as compounds containing isolated clusters with delocalized bonding[6] elude description by simple valence rules. Rather, the last group obey the Wade's rules developed for electron counting in deltahedral boranes, $B_nH_n^{2-}$. Examples of these are the metallic and also superconducting $AeSn_3$ (Ae = Sr, Ba), which may be explained as composed of triangular Sn_3^{2-} with delocalized three-center two-electron bonds,[7] the metallic Ae_3Tt_5 (Tt = Sn, Pb; Ae = Sr, Ba), which may be viewed as containing *arachno*-clusters of $[Tt_5]^{6-}$,[8] and the electron-balanced $Rb_4Li_2Sn_8$ with *arachno*-$[Sn_8]^{6-}$ as well as A_4Tt_9 and $A_{12}Tt_{17}$ (A = alkali

[a] S. Ponou, Prof. T. F. Fässler
Anorganisch-chemisches Institut
der Technischen Universität München
Lichtenbergstrasse 4, 85747 Garching (Germany)
Fax: (+49) 89-289-13186
E-mail: thomas.faessler@lrz.tum.de

[b] G. Tobías, Prof. E. Canadell
ICMAB-CSIC, Campus de la UAB
08193 Bellaterra (Spain)
E-mail: canadell@icmab.es

[c] A. Cho, Prof. S. C. Sevov
Department of Chemistry and Biochemistry
University of Notre Dame
Notre Dame, Indiana 46556 (USA)
E-mail: ssevov@nd.edu

Supporting information for this article is available on the WWW under http://www.chemeurj.org/ or from the author. One Figure showing anisotropic displacement parameters of the atoms and one Figure with sections of the Fermi surface of $Ba_5In_4Bi_5$.

DOI: 10.1002/chem.200306061

metal) with *nido*-$[Tt_9]^{4-}$.[6] More recent studies explored heteroatomic systems for clusters such as $[Tr_4Pn_5]^{3-}$, which are isoelectronic with $[Tt_9]^{4-}$. The advantage of such clusters is that it might be possible to vary their charge by changing the ratio between the two elements without changing the total number of atoms of the cluster, for example $[Tr_4Pn_5]^{3-}$ and $[Tr_5Pn_4]^{5-}$. Although no such clusters have been found in neat solids yet, they have been crystallized from ethylenediamine solutions of various ternary compounds $A_mTr_nPn_p$. Thus, $[In_4Bi_5]^{3-}$ has been characterized in [Na–crypt]$_3$[In_4Bi_5] (crypt = 4,7,13,16,21,24-hexaoxa-1,10-diazabicyclo-[8.8.8]-hexacosane.[9] The geometry of the cluster is similar to that of $[Tt_9]^{4-}$ and can be described as a distorted monocapped square antiprism in which the four indium atoms occupy the five bonded positions (Scheme 1). The synthesis of the same or similar heteroatomic clusters with delocalized bonding in the solid state has been elusive so far despite the intensive efforts. Instead, reactions designed to produce such clusters have provided various Zintl phases with extended structures of corner- and/or edge-shared $TrPn_4$ tetrahedra and with localized bonding.

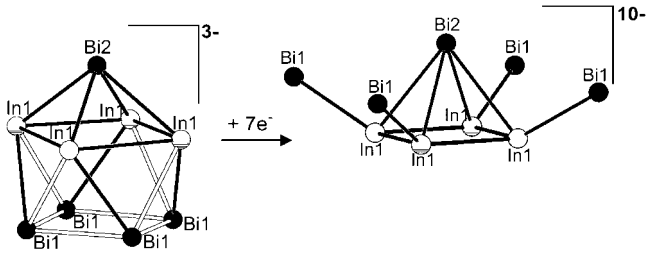

Scheme 1.

Here we report the synthesis, structure, and electronic structure of a phase, $Ba_5In_4Bi_5$, in which both localized and delocalized bonding can be found. It can be described as containing isolated forms of the same composition as the clusters crystallized from solution, $[In_4Bi_5]$, but with different charge, $[In_4Bi_5]^{10-}$. Furthermore, according to calculations, this charge is one electron short from the corresponding closed-shell species, that is, $[In_4Bi_5]^{11-}$.

Results and Discussion

The new compound $Ba_5In_4Bi_5$ crystallizes in the noncentrosymmetric space group *P*4*nc* and presents a new structure type according to a single-crystal structure determination. Details of the data collection and refinement are given in Table 1, while the atomic positions and important interatomic distances are listed in Tables 2 and 3, respectively. The structure contains square pyramids with four *exo*-bonds at the square base (idealized C_{4v} symmetry). The base is made of the four indium atoms, while the four *exo*-bonded atoms (Bi1) and the apex of the pyramid (Bi2) are the five bismuth atoms (Figure 1).

Table 1. Crystallographic data and structure refinement of $Ba_5In_4Bi_5$.

formula	$Ba_5In_4Bi_5$	reflection measured	8204
M_r	2190.88	independent reflections	1137
space group	*P*4*nc* (no. 104)	observed reflections [$I>2\sigma(I)$]	1046
T [K]	293(2)	R_{int}/R_σ	0.0584/0.0339
λ [Å]	0.71073	absorption correction	numerical
a [Å]	10.620(1)	min/max transmission	0.0135/0.0967
c [Å]	9.009(2)	Parameters	35
V [Å^3]	1016.0(3)	goodness-of-fit on F^2	1.219/1.219
Z	2	R_1/wR_2[a] [$I>2\sigma(I)$]	0.0237/0.0700
ρ_{calcd} [g cm^{-3}]	7.161	R_1/wR_2, all data	0.0273/0.0843
μ [cm^{-1}]	570.39	Flack parameter	−0.07(1)
F(000)	1782	extinction parameter	0.0067(3)
2θ range [°]	3.8–55.7	largest diff peak and hole [e Å^{-3}]	3.32/−2.64
index ranges	$-13\le h\le 13$		
	$-13\le k\le 13$		
	$-11\le l\le 11$		

[a] $R_1(F_o)=\Sigma[\,|F_o|-|F_c|\,]/\Sigma|F_o|$; $wR_2=\{\Sigma[w(F_o^2-F_c^2)^2]/\Sigma[w(F_o^2)^2]\}$; $w=1/[\sigma^2(F_o^2)+(0.0382P)^2+28.60P]$ in which $P=(\mathrm{Max}(F_o^2,0)+2F_c^2)/3$.

Table 2. Atomic coordinates and isotropic equivalent displacement parameters.

Atom	Site	x	y	z	U_{eq} [Å^2]
Bi1	8*c*	0.39058(7)	0.19079(7)	0.69032(8)	0.0175(3)
Bi2	2*a*	0.5	0.5	0.3180(2)	0.0123(4)
Ba1	8*c*	0.6057(2)	0.1884(2)	0.3740(2)	0.0170(4)
Ba2	2*a*	0.5	0.5	0.7001(3)	0.0210(6)
In1	8*c*	0.1834(2)	0.0720(2)	0.5316(2)	0.0200(4)

Table 3. Selected interatomic distances [Å].

Bi1–In1	2.912(2)	In1–In1	2.958(2) ×2
Bi1–In1	3.376(2)[a]	In1–Ba1	3.707(2)
Bi1–Ba1	3.653(2)	In1–Ba1	3.830(2)
Bi1–Ba1	3.655(2)	In1–Ba1	3.864(2)
Bi1–Ba1	3.679(2)	In1–Ba1	4.084(2)
Bi1–Ba1	3.682(2)	Ba2–Bi1	3.484(1) ×4
Bi1–Ba1	4.171(2)	Ba2–In1	3.647(2) ×4
Bi2–In1	3.322(2) ×4		
Bi2–Ba2	3.442(3)		
Bi2–Ba1	3.531(2) ×4		

[a] Intercluster bonds.

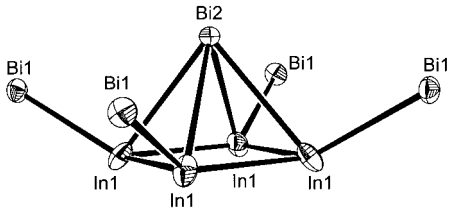

Figure 1. $[In_4Bi_5]$ cluster in $Ba_5In_4Bi_5$ (thermal ellipsoids at the 70% probability level).

The In–Bi *exo*-bond length of 2.912(2) Å is quite normal for a single bond between these elements. It compares well, for example, with the observed range of distances in $Cs_7In_4Bi_6$, 2.896(3)–3.105(3) Å.[3b] The In–In distance in the square, 2.958(2) Å, is also close to a single-bond length, when compared with 2.976(4) and 3.004(5) Å observed between indium atoms coordinated by bismuth in $Cs_7In_4Bi_6$.[3b] Nevertheless, it is somewhat longer than the Pauling's distance for a single bond, 2.84 Å.[10] The remaining four In–Bi distances in the pyramid, that is, those to the apical Bi atom, are quite long for a single bond, 3.322(2) Å, and suggest rather delocalized bonding. They compare better with the intercluster distances of 3.376(2) Å that occur between the *exo*-bonded bismuth atoms and indium atoms of four neighboring pyramids (Figure 2). This suggests that the interactions between the pyramids can not be disregarded. Thus, the clusters should not be considered as isolated units but rather as parts of an extended network as shown in Figure 2.

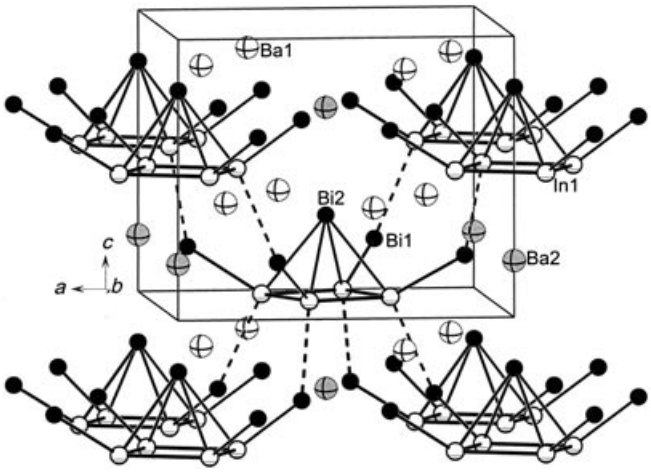

Figure 2. The structure of $Ba_5In_4Bi_5$ with the unit cell outlined (Ba1: crossed circle, Ba2: gray crossed, Bi: black, In: open shaded). The square pyramidal clusters with four *exo*-bonds are stacked along the *c* axis. They are connected by longer Bi–In distances shown as black dotted lines.

The five barium cations in the formula occupy two different positions. Ba2 caps the square base of the In_4Bi pyramid (opposite to the Bi apex) with Ba–In distances of 3.647(2) Å (Figure 3). Its coordination environment is very similar to that of the capping bismuth atom, Bi2, and resembles a pseudo-octahedron in which one of the vertices is replaced by the In_4 square (Figure 3). Thus the nearest neighbors of Bi2 and Ba2 are ($4\,Ba1 + Ba2 + \eta^4$-In_4) and ($4\,Bi1 + Bi2 + \eta^4$-In_4), respectively. It is perhaps these structural reciprocities that give rise to the observed substantial contribution of barium in the calculated electronic structure of the compound (below). Also, if we consider Ba2 as part of the cluster, we obtain an octahedral unit surrounded by Bi and Ba atoms that bridge edges and cap faces and resemble the coordination topology of the well-known M_6X_{18} clusters (Figure 3). Ba1, on the other hand, has twelve neighbors

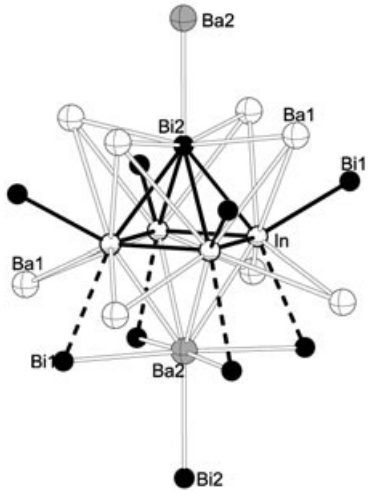

Figure 3. A closer view of the coordination around $[In_4Bi_5]$ showing an octahedron-like formation capped by Ba2 and Bi1 that resembles M_6X_{18} clusters (Bi: black, Ba1: crossed, Ba2: gray crossed, In1: gray). All Ba–In and Ba–Bi interactions are shown with open bonds. The similarity of the coordinations of Ba2 and Bi2 is clearly visible.

($Bi2 + 5\,Bi1 + 4\,In1 + Ba2 + Ba1$), an indication for less directional interactions.

The *exo*-bonded square pyramids are stacked in columns along the *c* axis (Figure 2) and the columns are connected through the intercluster In–Bi distances of 3.376(2) Å (above). Neighboring columns are shifted by *c*/2 with respect to each other and are also rotated by approximately 16.4° with respect to each other around the *c* axis. The rotation reduces the overall symmetry of the cell from body-centered to the current tetragonal primitive unit cell. The occurrence of such a rotation originates most likely from a strong need for the clusters to interlink to each other.

Full electron transfer from barium to the more electronegative indium and bismuth as prescribed by the Zintl–Klemm concept would result in a charge of −10 for the *exo*-bonded pyramid, that is, $[In_4Bi_5]^{10-}$. On the other hand, the species can be viewed as composed of a deltahedral *nido*-cluster with $2n + 4 = 14$ skeletal bonding electrons: four two-center two-electron *exo*-bonds, one lone pair of electrons at the apical bismuth, and four *exo*-bonded bismuth atoms that need another six electrons each in order to satisfy the octet rule. This totals $14 + 8 + 2 + 24 = 48$ electrons, of which only 37 are provided by the four In (3 electrons each) and five Bi (5 electrons each) atoms. Thus, a closed-shell species should have a charge of −11 instead, that is, $[In_4Bi_5]^{11-}$; therefore $[In_4Bi_5]^{10-}$ is one electron short. It should be pointed out here that the previously known deltahedral cluster with the same stoichiometry $[In_4Bi_5]^{3-}$ has substantially different charge and very different geometry.[9] It is a closed-shell *nido*-cluster of nine atoms with the shape of a monocapped square antiprism as shown in the left of Scheme 1. With respect to this, the new species $[In_4Bi_5]^{10-}$ can be viewed as its inverted, opened version, almost as the blossomed flower from its bud of $[In_4Bi_5]^{3-}$. This "process" during which some In–Bi and Bi–Bi interactions are formally removed is clearly caused by the substantial reduction with seven additional

electrons (eight electrons for a closed-shell unit of $[In_4Bi_5]^{11-}$) that would fill four empty antibonding levels of the cluster. This, as can be expected, leads to a major reorganization of the delocalized bonding within the cluster that is expressed in the removal of the four Bi–Bi interactions at the open square face of $[In_4Bi_5]^{3-}$ as well as four of the associated Bi–In bonds, while reinforcing the four remaining Bi–In bonds. The four bismuth atoms are then shifted upwards and also tangentially away from one of the two indium atoms to which they are bonded. Apparently, this tangential displacement of the bismuth atoms is not complete, and they are not perfectly radial with respect to the cluster, but are rather 7.4° off of the vertical plane through In-Bi2-In. Thus, although the In_4Bi pyramid has exact C_{4v} symmetry, the symmetry of the whole unit $[In_4Bi_5]^{10-}$ is reduced to C_4.

In order to gain some insight into the factors behind the stability of this apparently one-electron-deficient compound, first principle DFT calculations were carried out. The calculated band structure along the main symmetry lines of the tetragonal Brillouin zone (Figure 4) shows a group of four bands near the Fermi level that are flat along Γ-M-X-Γ (the *ab* plane), but are dispersed along Γ-Z-A-M (perpendicular to the *ab* plane). This indicates that these bands are involved in interactions only along the *c* axis. There is also an additional, very dispersed band that goes along Γ→X, Γ→M, and Γ→Z, and overlaps with the set of four flat bands (Figure 4). This band has In–Bi antibonding character, but is stabilized by mixing with barium states, specifically through Ba–Bi bonding interactions. The Fermi level passes through the four flat bands (and the bottom of the dispersed band) and makes them partially filled. They would have been completely filled with two additional electrons in a hypothetical, electronically balanced compound "$Ba_{11}In_8Bi_{10}$" (note that the unit cell contains two formula units). The continuum of states at and around the Fermi level is consistent with the observed metallic properties. However, due to the dispersed Bi–In antibonding band, there is no band gap even for the hypothetical compound "$Ba_{11}In_8Bi_{10}$" with two additional electrons.

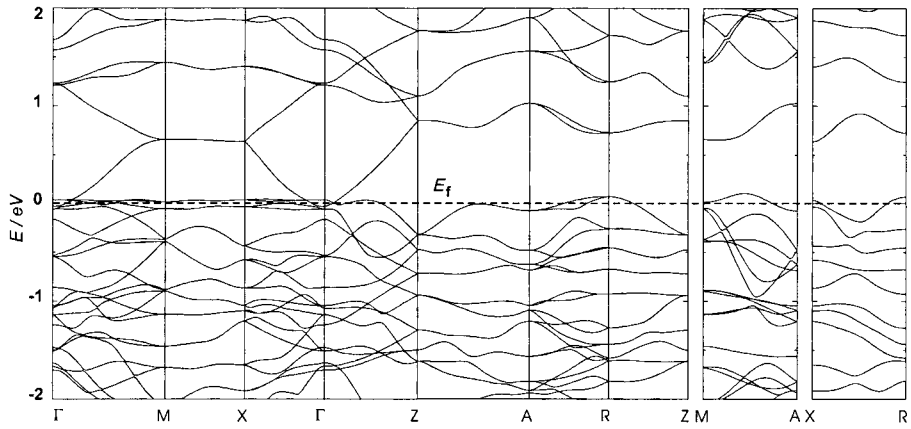

Figure 4. Calculated band structure for $Ba_5In_4Bi_5$ (Γ = 0, 0, 0; X = 1/2, 0, 0; M = 1/2, 1/2, 0; Z = 0, 0, 1/2; R = 1/2, 0, 1/2; A = 1/2, 1/2, 1/2, in units of the tetragonal reciprocal lattice vectors).

The orbital nature of the bands indicates that barium has substantial contribution in many of the filled bands and should not be considered simply as an electron donor for the Bi–In bonding, but rather as an important participant in the overall bonding of the structure. This is reflected in the calculated Mulliken charges of +0.28 and +0.38 for barium; that is, quite different from the expected +2 for complete electron transfer. The overlap populations are also very informative. For In–In this is 0.279, while the values for In–Bi are 0.292 for the *exo*-bond, 0.102 within the pyramid, and 0.134 for the inter-unit interaction. Of course, the more interesting values are those for the Ba–Bi contacts, and they are +0.152 (×4) and +0.097 for the five neighbors around Bi2 and +0.139, +0.117, +0.123, +0.108, and +0.122 for the five neighbors of Bi1. These positive and larger than 0.1 values indicate substantial Ba–Bi bonding interactions and are consistent with the observed large Ba contribution in the filled DOS (see Figure 5; DOS = density of states). Therefore, the structure of $Ba_5In_4Bi_5$ should be viewed as a three-dimensional network of Ba-Bi-In, in which the Ba–Bi bonding interactions contribute significantly to the cohesion energy of the system (there seem to be no bonding Ba–In interactions). Thus, based on all these observations, it can be concluded quite firmly that barium plays an essential role in the covalent bonding of the structure. A similar situation has been recently suggested for phases like K_5Bi_4 and K_3Bi_2.[11]

Further analysis of the electronic structure of $Ba_5In_4Bi_5$ was done based on the calculated total DOS of the compound and the separate contributions from the constituting elements (Figure 5). The four peaks with the lowest energies in the DOS are the bismuth and indium s orbitals. The continuous region following them (−3.5 to 0.2 eV) contains predominantly contributions from the p orbitals of Bi and In, but also non-negligible participation from Ba. As a matter of fact, the latter is more than 30% and is almost as large as that of indium. For two-thirds of this block (−3.5 to −1.0 eV) the In and Bi contributions have very similar shapes (the curves follow each other) and indicate good Bi–In orbital mixing and bonding interactions. The remaining one-third of the block is dominated by the bismuth p orbitals, particularly from p_z orbitals. The sharp spike right at the Fermi level is almost purely bismuth p_z orbitals, mostly from Bi1, that would have been filled if two additional electrons were available. This peak is made of the four flat bands discussed above and has essentially nonbonding character; therefore, the predominant character of the "missing" two electrons would have been nonbonding.

Because there is one missing electron per formula unit, the Fermi level cuts bands which are flat along certain direc-

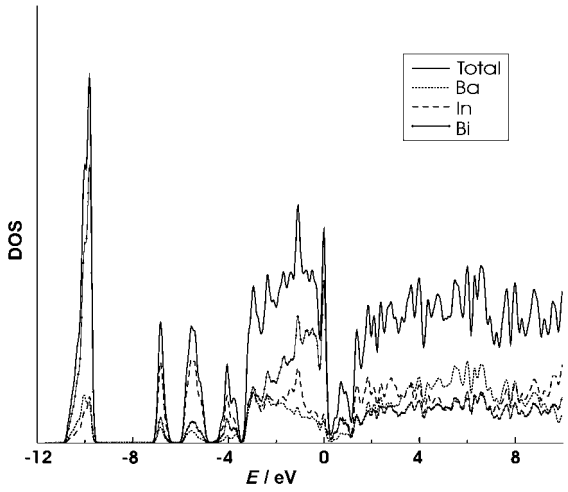

Figure 5. Total and projected density of states of $Ba_5In_4Bi_5$

tions but not along others. In principle a situation in which a single electron per formula unit remains localized is also an alternative possibility. In that case the phase could be a magnetic insulator. In order to test this possibility we also carried out spin-polarized calculations for $Ba_5In_4Bi_5$. These calculations led to exactly the same result as those without spin polarization. Thus we conclude that the present phase should be a metal with a high density of states at the Fermi level. The calculated Fermi surface (see Supporting Information), as can be expected from the nature of the bands at the Fermi level, is extremely complex with many electron and hole pockets of different sizes. This is the signature of a good three-dimensional metal. The absence of nesting features in the Fermi surface makes the phase immune to density-wave-type instabilities,[12] and the compound is predicted to remain metallic even at very low temperatures. Also, the fact that the Fermi level passes near a maximum in the density of states suggests that the compound could be superconducting. However, all tests at temperatures as low as 2 K and various fields on both field cooled and zero-field cooled samples gave negative results and did not show superconducting transitions.

As already discussed, $Ba_5In_4Bi_5$ presents a very well packed structure with matching positioning for the five barium and five bismuth atoms with respect to each other, as well as with respect to the indium square. Thus, barium is in positions that allow optimum interactions with the nonbonding lone pairs of both the capping Bi2 and the four *exo*-bonded Bi1 atoms. Therefore, although the anionic part of the structure, that is, Bi−In, does not have enough electrons to fill the relatively high-lying levels (mostly Bi) near the Fermi level, the overall structure, that is, Ba-In-Bi, compensates this by switching on relatively strong Ba−Bi bonding interactions and thus stabilizing a considerable portion of the filled DOS. What makes it difficult to understand structures like this one is our biased way of looking at the structures of polar intermetallic compounds as built of an anionic, covalently-bonded substructure of the p elements and isolated cations of the s elements that only provide electrons. What the present study suggests is, that if it is impossible to find room for all cations necessary for electron balancing in a particular structure, the system finds such a distribution of the available cations that would maximize their participation in the covalent bonding of the structure and thus compensate for the electron "deficit". A related explanation holds for phases with extra electrons.[11,14]

Electron-deficient compounds are very rare and only a few precedents are known. K6Sn25 is electron deficient due to lone pair interactions.[15] The two most recent examples, Sr_3In_5 and K_2SrIn_7,[16] are both with extended indium networks and are also one-electron short for closed-shell compounds. Similar to $Ba_5In_4Bi_5$ they should be viewed as structures stabilized by cation–anion interactions that compensate for the missing bonding electrons. Apparently such electron "shortages" with respect to the classical closed-shell bonding schemes can develop when other factors such as Madelung energy and packing efficiency become perhaps more important than covalent bonding. $Ba_5In_4Bi_5$ presents the first such an example that involves a heteroatomic framework. In this case, the "decisive" factor appears to be the substantial participation of Ba in the overall bonding of the structure.

Experimental Section

Synthesis: All manipulations were performed inside argon-filled glove boxes with moisture levels below 1 ppm. The new compound was synthesized from the elements (at Notre Dame: all from Alfa-Aesar, 99.95+ % purity; at Darmstadt/Munich: all from Chempur, Bi 99.99 %, In 99.99 %, and Ba 99.3 %). Typically, a mixture of them was loaded in a niobium container that was then sealed by arc-welding under argon at low pressure. The container was in turn enclosed in an ampoule made of fused-silica, and after evacuation the latter was flame-sealed. The assembly was heated in tubular furnace with temperature control. Initially $Ba_5In_4Bi_5$ was characterized as one of the products of two different reactions: at Notre Dame the used molar ratio of Ba/In/Bi was 3:2:4 and the mixture was heated at 700 °C for 10 days and slowly cooled to room temperature at a rate of 6 °C h^{-1}, while at Darmstadt/Munich the corresponding molar ratio of the elements was 2:3:3 (designed to produce an eventual intergrowth structure of $BaBi_3$ and $BaIn_3$ to be isoelectronic with the known $BaSn_3$[7]) and the mixture was then heated at 800 °C for 5 h, cooled down to 400 °C with a rate of 60 °C h^{-1}, and held at that temperature for five days before cooling to room temperature. The latter reaction yielded $Ba_5In_4Bi_5$ and traces of amorphous phase (according to powder X-ray diffraction). Pure phase was later made from the corresponding stoichiometric composition. The compound was air-sensitive and crystallized as irregular silver crystals with a metallic luster. Energy-dispersive X-ray (EDX) spectroscopic analysis confirmed the presence of all three elements and absence of possible niobium impurities or any other elements.

Structure determination: Crystals of $Ba_5In_4Bi_5$ were selected, mounted in thin-wall glass capillaries, and checked for singularity. The best one, a needle-shaped single crystal ($0.40\times0.167\times0.05$ mm), was used for data collection at 23 °C with a Stoe IPDS (image plate detector system) diffractometer with monochromated $Mo_{K\alpha}$ radiation (180 frames with exposure time of 7 min per frame, angular range of $3.8° < 2\theta < 55.7°$, ω-scans, $\Delta\omega = 1°$. Numerical absorption correction was applied by using the program X-shape from STOE[29]). The structure was solved (direct methods) and refined (on F^2) in the acentric $P4nc$ space group with the aid of the SHELXTL-V5.1 software package.[17] Further details of the crystal structure investigation can be obtained from Fachinformationszentrum Karlsruhe, 76344 Eggenstein-Leopoldshafen, Germany (fax: (+49) 7247–808–666; e-mail: crysdata@fiz-karlsruhe.de) on quoting the depository number CSD-413581.

Magnetic measurements: The magnetization of 48.3 mg of $Ba_5In_4Bi_5$ was measured on a Quantum Design MPMS SQUID magnetometer at a field of 3 T over the temperature range 10–250 K. The sample was made by manual selection of large crystals only in order to ensure absence of any small impurities. These were then coarsely ground and sealed in fused-silica tubing (I.D. = 3 mm) between two tightly fitting rods of the same material. The raw data were corrected for the holder and for the ion-core diamagnetism of $5\,Ba^{2+}$, $4\,In^{3+}$, and $5\,Bi^{5+}$. The resulting molar magnetic susceptibility was positive and temperature independent, $+(4.8$ to $6.6)\times 10^{-4}$ emu mol^{-1} ($+3.5\times 10^{-4}$ emu mol^{-1} for a second sample). This is consistent with Pauli-type paramagnetism that is associated with metallic properties. Samples were also tested for superconductivity down to 2 K at fields of 500 and 100 Oe, both at zero-field cooled and field cooled conditions, but none of them showed such a transition.

Conductivity measurements: A four-probe device (in-line head from JANDEL with 1 mm spacing), set up inside a nitrogen-filled glove box with a cold trap, was used to measure the temperature dependence of the resistivity of $Ba_5In_4Bi_5$. A thin pellet of the compound with thickness of 0.26 mm was used as a sample (35 mg). The assembly was placed inside the cold trap and the latter was cooled externally with liquid nitrogen. Due to the apparent high conductivity of the compound the maximum possible current of 10000 μA available from the JANDEL RM2 unit was used. Despite this, however, the voltage that was measured was still nearly zero, between 0.06 and 0.07 mV, and its variation with the temperature was out of the range of the measuring unit. Thus, using these measured values the resistivity is calculated to be $825\times 10^{-8}\,\Omega$m ($236\times 10^{-8}\,\Omega$m for a second sample), that is, a highly conducting compound. For comparison, the resistivities of elemental Mn and $Yb_{14}MnSb_{11}$ are 144×10^{-8} and ca. $1100\times 10^{-8}\,\Omega$m, respectively.[18]

Band structure calculations: The calculations were carried out by using a numerical atomic orbitals DFT approach.[19,20] This method, developed relatively recently, is designed for efficient calculations in large systems and implemented in the SIESTA code.[21] The use of atomic orbitals instead of plane waves greatly facilitates a chemical analysis of the results. We used the local density approximation to DFT and, in particular, the functional of Perdew and Zunger.[22] Following recent first-principles work on bismuth-containing intermetallics,[23] only the valence electrons were considered in the calculation, with the core being replaced by norm-conserving scalar relativistic pseudopotentials factorized in the Kleinman–Bylander form.[24,25] Nonlinear partial-core corrections to describe the exchange and correlations in the core region were included.[26] We used a split-valence double-ζ basis set including polarization orbitals for all atoms, as obtained with an energy shift of 250 meV.[27] The integrals of the self-consistent terms of the Kohn–Sham Hamiltonian were obtained with the help of a regular real space grid in which the electron density was projected. The grid spacing was determined by the maximum kinetic energy of the plane waves that can be represented in that grid. In the present work, we used a cut off of 150 Ry. The Brillouin zone (BZ) was sampled by using a grid of $(5\times 5\times 5)$ k points.[28] We checked that the results were well converged with respect to the real space grid, the BZ sampling, and the range of the atomic orbitals.

Acknowledgments

This work was partially supported by funding from the National Science Foundation (Grant CHE-0098004), DGI-Spain (Project BFM2000–1312-C02–01), and Generalitat de Catalunya (Project 2001 SGR 333). G.T. acknowledges support from the Ministerio de Ciencia y Tecnología of Spain. The computations were carried out using the resources of CESCA and CEPBA. S.P. and T.F.F. thank the European Union for support within the RTN program (EU-project Nr. HPRN-CT 2002-00193).

[1] a) E. Zintl, *Angew. Chem.* **1939**, *52*, 1; b) W. Klemm, *Proc. Chem. Soc. London* **1958**,329.
[2] a) B. Eisenmann, G. Cordier in *Chemistry, Structure and Bonding of Zintl Phases and Ions* (Ed.: S. M. Kauzlarich), VCH, Weinheim, **1996**, p. 61; b) F. Gascoin, S. C. Sevov, *Inorg. Chem.* **2002**, *41*, 2292.
[3] a) G. Cordier, H. Ochmann, H. Schafer, *Mater. Res. Bull.* **1986**, *21*, 331; b) S. Bobev, S. C. Sevov, *Inorg. Chem.* **1999**, *38*, 2672; c) S. Bobev, S. C. Sevov, *J. Solid State Chem.* **2002**, *163*, 436; d) F. Gascoin, S. C. Sevov, *Inorg. Chem.* **2001**, *40*, 6254; e) S.-J. Kim, M. G. Kanatzidis, *Inorg. Chem.* **2001**, *40*, 3781; f) S.-M. Park, S.-J. Kim and M. G. Kanatzidis, *J. Solid State Chem.* **2003**, *174*, 310.
[4] a) S. M. Kauzlarich in *Chemistry, Structure and Bonding of Zintl Phases and Ions* (Ed.: S. M. Kauzlarich), VCH, **1996**, p. 245; b) F. Gascoin, S. C. Sevov, *Inorg. Chem.* **2003**, *42*, 904.
[5] a) F. Gascoin, S. C. Sevov, *Inorg. Chem.* **2002**, *41*, 5920; b) F. Gascoin, S. C. Sevov, *Inorg. Chem.* **2003**, *42*, 8567; c) A. S. Sefat, J. E. Greedan, *Inorg. Chem.* **2004**, *43*, 142.
[6] a) V. Quenéau, S. C. Sevov, *Angew. Chem.* **1997**, *109*, 1818; *Angew. Chem. Int. Ed. Engl.* **1997**, *36*, 1754; b) V. Quenéau, E. Todorov, S. C. Sevov, *J. Am. Chem. Soc.* **1998**,*120*, 3263; c) V. Quenéau, S. C. Sevov, *Inorg. Chem.* **1998**, *37*, 1358; d) E. Todorov, S. C. Sevov, *Inorg. Chem.* **1998**, *37*, 3889; e) H.-G. v. Schnering, M. Baitinger, U. Bolle, W. Carrillo-Cabrera, J. Curda, Y. Grin, F. Heinemann, J. Llanos, K. Peters, A. Schmeding, M. Somer, *Z. Anorg. Allg. Chem.* **1997**, *623*, 1037; f) S. Bobev, S. C. Sevov, *Angew. Chem.* **2000**, *112*, 4274; *Angew. Chem. Int. Ed.* **2000**, *39*, 4108; g) S. Bobev, S. C. Sevov, *Polyhedron* **2002**, *21*, 641.
[7] a) T. F. Fässler, C. Kronseder, *Angew. Chem.* **1997**, *109,* 2800; *Angew. Chem. Int. Ed. Engl.* **1997**, *36*, 2683; b) T. F. Fässler, S. Hoffmann, *Z. Anorg. Allg. Chem.* **2000**, *626*, 106.
[8] F. Zurcher, R. Nesper, S. Hoffmann, T. F. Fässler, *Z. Anorg. Allg. Chem.* **2001**, *627*, 2211.
[9] L. Xu, S. C. Sevov, *Inorg. Chem.* **2000**, *39*, 5383.
[10] L. Pauling, *The Nature of the Chemical Bond*; Cornell University Press, Ithaca, NY, **1960**.
[11] A. Rodríguez-Fortea, E. Canadell, *Inorg. Chem.* **2003**, *42*, 2759; P. Alemany, E. Canadell, unpublished results.
[12] E. Canadell, M.-H. Whangbo, *Chem. Rev.* **1991**, *91*, 965.
[13] T. A. Albright, J. K. Burdett, M.-H. Whangbo, *Orbital Interactions in Chemistry*, Wiley, New York, **1985**.
[14] B. Li, L. Chi, J. D. Corbett, *Inorg. Chem.* **2003**, *42*, 3036.
[15] T. F. Fässler, *Z. Anorg. Allg. Chem.* **1998**, *624*, 569.
[16] a) D. -K. Seo, J. D. Corbett, *J. Am. Chem. Soc.* **2001**, *123*, 4512; b) L. Chi, J. D. Corbett *Inorg. Chem.* **2001**, *40*, 3596.
[17] Bruker Analytical X-ray Systems, Inc., Madison, WI, **1997**.
[18] a) *CRC Handbook of Chemistry and Physics*, 81st ed., CRC, New York, **2001–2002**, Section 12, p. 47; b) I. R. Fisher, T. A. Wiener, S. L. Bud'ko, P. C. Canfield, J. Y. Chan, S. M. Kauzlarich, *Phys. Rev. B* **1999**, *59*, 13829.
[19] P. Hohenberg, W, Kohn, *Phys. Rev.* **1964**, *136*, 864.
[20] W. Kohn, L. J. Sham, *Phys. Rev.* **1965**, *140*, 1133.
[21] J. M. Soler, E. Artacho, J. D. Gale, A. García, J. Junquera, P. Ordejón and D. Sánchez-Portal, *J. Phys. Condens. Matter* **2002**, *14*, 2745 .
[22] J. P. Perdew, A. Zunger, *Phys. Rev. B* **1981**, *23*, 5075.
[23] D. Sánchez-Portal, R. M. Martin, S. M. Kauzlarich, W. E. Pickett, *Phys. Rev. B* **2002**, *65*, 144414.
[24] N. Trouiller, J. L. Martins, *Phys. Rev. B* **1991**, *43*, 1993.
[25] L. Kleinman, D. M. Bylander, *Phys. Rev. Lett.* **1982**, *48*, 1425.
[26] S. G. Louie, S. Froyen, M. L. Cohen, *Phys. Rev. B* **1982**, *26*, 1738.
[27] E. Artacho, D. Sánchez-Portal, P. Ordejón, A. García, J. M. Soler, *Phys. Status Solidi B* **1999**, *215*, 809.
[28] H. J. Monkhorst, J. D. Park, *Phys. Rev. B* **1976**, *13*, 5188.
[29] Fa. STOE Darmstadt, Program X-SHAPE: Crystal Optimisation for Numerical Absorption Correction 1.01, **1996**.

Received: December 22, 2003
Published online: May 25, 2004

